RECD- SEPT 22, 1941

3

NATIONAL ADVISORY COMMITTEE FOR AERONAUTICS

CLASSIFICATION CANCELLED

RESTRICTED

NOT EDITED

CASE FILE COPY

CLASSIFICATION CANCELLED

ADVANCE RESTRICTED REPORT

FLIGHT TESTS OF THE

WILFORD XOZ-1 SEA GYROPLANE

By Frederic B. Gustafson

CLASSIFICATION CANCELLED

Authority Aeronautical Bd. Date 4/4/46

By OES

FILE COPY
To be returned to
the files of the National
Advisory Committee
for Aeronautics
Washington, D. C.

September 12, 1941

Enclosure (1) BuAer ltr Aer-TD-416/386
of

ADVANCE RESTRICTED REPORT

FLIGHT TESTS OF THE WILFORD XOZ-1 SEA GYROPLANE

By FREDERIC B. GUSTAFSON

INTRODUCTION

During August 1939 a series of flight tests was made at Langley Field on the Wilford sea gyroplane, designated by the Navy as the XOZ-1. These tests were intended to permit rough evaluation of the stability and control characteristics of the machine, with particular reference to possible improvements in rigging which might be made in future machines with fixed wing and nonarticulated feathering-control rotor, and to provide data on the bending and feathering motions of the rotor blades.

The tests made in 1939 proved inadequate, chiefly because the machine as flown did not have sufficient propeller thrust to give it an appreciable speed range in steady flight. Further tests were therefore made in August 1940 after overhauling the engine and substituting a metal propeller for the wooden one first used. The range of speeds covered in steady flight was markedly extended. Steady-flight runs only were made in this series, since it was felt that take-offs and landings had been covered sufficiently in the previous tests.

APPARATUS

The XOZ-1 is a converted fleet trainer, placed on Edo floats and rigged with a four-blade rotor in place of the upper wing. The rotor of the XOZ-1 differs basically from all other available rotors in that it is nonarticulated, that is, bending stresses in the spars are not relieved by hinges. Balance and control are achieved by feathering the blades, substantially about their span axes. Elevators, stabilizer, ailerons, and rudder are retained. The elevators and ailerons are interlocked with the rotor control in the manner shown in figure 1. It may be noted that the feathering has a 30° "lead" and that, allowing for this lead, with the ailerons and elevators in midposition the feathering is zero fore and aft and 1.6° laterally.

The gyroplane as flown was equipped with a four-blade rotor with a diameter of 30 feet. The area of the fixed wing, exclusive of the fuselage, is 110 square feet; rotor disk area is 707 square feet. The wing section used in the wing is the Clark Y, and in the rotor blades, the NACA 2418. Blade plan form is rectangular with eliptical tips. The blades were set at 0.8° pitch during these tests. The fixed wing was rigged with a slight twist and at a small positive angle of attack relative to the plane of the rotor. Measurements at the time of these flights gave the following values for the angle between the thrust axis and the lower

sides of the wing spars: left wing at second rib from tip, 1.9°; left wing at third rib from root, 2.6°; right wing at third rib from root, 3.1°; right wing at second rib from tip, 2.9°. The wing chord has an angle about 0.7° lower than that which the spars give. The rotor is mounted at an angle of 1° to the thrust axis.

Rotor-blade motion, including blade angle at the 0.75 radius and blade deflection in bending, was recorded by means of a moving-picture camera mounted on the top of the rotor hub. The blade angle was obtained by the use of metal targets extending from the leading and trailing edge at the 0.75 radius. Blade deflection at the tip was determined from a small metal target. The ends of black paint stripes were used as targets at the following fractions of the radius to enable determination of deflections at these points: 0.375, 0.500, 0.625, 0.75, and 0.875. In order to permit a comparison of blade-section stalling on this rotor with that on other rotors tested (reference 2), short pieces of wool yarn were attached at 30, 40, 50, 62.5, and 75 percent of the blade radius.

Control and stability data were obtained by means of the following recording instruments: control-force recorder, control-position recorder, and inclinometer. A recording tachometer was used to obtain rotor speed and a recording airspeed unit was connected to a swiveling pitot head.

TESTS AND PROCEDURE

In the course of the 1940 tests, records were obtained during three separate flights. During the first flight only four records were obtained. The camera and tachometer failed to work; hence the data obtained are not included in this report, although they were available for comparison with the subsequent records. During the fourth and last run of this flight, the rotor suddenly became rough, and during the subsequent landing and taxying, which were in rougher water than usual, a heavy shake in the control stick and a weaving in the pylon were noted. A speed of 74 miles an hour was reached in this last run. It was found that bolts at the top of the pylon structure had loosened, much as bolts at the bottom of the pylon had done during the tests of the previous year. New bolts were fitted and no further trouble of this nature was encountered during the rather limited time the ship was flown. During the second flight, the camera functioned but the control-position recorder and the tachometer did not. Thirteen separate records were obtained covering the speed range of the machine. It was found possible to determine the rotor rpm quite accurately from oscillations on the inclinometer records; hence the camera records were worked up and used, as were the remaining instrument records. In the third flight, all instruments and the camera functioned and again 13 records were taken. The procedure used was to take six or seven records at

successively higher airspeeds up to the maximum, and then to take the remainder at successively lower speeds down to the lowest obtainable with reasonably constant speed. While it was not possible to obtain truly steady level flight at speeds below 50 miles per hour, by reason of insufficient power, records were taken and used for speeds as low as 39 miles per hour.

In analyzing the camera records, azimuth angles were determined first by means of the spots left by the timing device. Use was made of the presence of fairly clear horizons in the pictures; both the horizon elevation and the horizon angle, when suitably plotted, will yield azimuth values for the various pictures. Azimuths obtained by studying the horizons were averaged with those from the timing marks.

Blade deflection at the various radii was based on readings taken with the blade still and unsupported. Deflection on the film was converted into inches of spar deflection by means of constants obtained by taking still pictures with a ruler set at each of the several radii. The effect of blade feathering on spar height, which results from the sweepback present, was corrected for by means of the blade-angle reading. A slight error, considered negligible, is introduced by the existence of a small periodic twist in the blades.

Feathering angles at the 0.75 radius were determined by readings from the appropriate targets, corrected for the difference between the angle read for the image of the targets with the blade at rest and the 0.8° pitch setting of the blade. In obtaining the correction, the stick was held fixed at approximately neutral, pictures were taken with the blade in four positions 90° apart, and 0.8° subtracted from the average of these four readings. All readings were referred to the edge of the corresponding picture.

In analyzing the records from the various instruments, it was usually necessary to read mean values rather than instantaneous values. In the case of the control-force recorder, an instrument of different characteristics would have to be used in order actually to measure the stick-vibration forces, and it is only possible to conclude from this record that they were not particularly large; this was checked by the pilot's statement that the stick vibration resembled that in an airplane. In the case of the inclinometer, the readings plotted in such erratic fashion that more dependence is placed on values determined from the horizon-angle readings obtained from the camera records.

RESULTS

Fourteen of the runs gave records which were suitable for blade bending and feathering studies. Figure 2 is a sample of the manner in which the corrected bending-deflection data were plotted. These plots were used as a basis for harmonic analysis from which (1) the average bending or coning deflection, (2) the magnitude of the various harmonics which combine to represent the periodic blade motion, and (3) the phase angle in azimuth of these harmonics were determined. The harmonic analysis is based on the equation

$$\beta = a_o + a_1 \cos \psi + b_1 \sin \psi + a_2 \cos 2 + b_2 \sin 2 \psi + \ldots$$

where the symbols differ from those in reference 1 in that β and the various coefficients represent deflection in inches at the tip and not angular displacement. Figure 3 shows the coning deflection plotted against tip-speed ratio. The highest and lowest points of the faired bending cycles, of which figure 2 is an example, are also shown on this figure. Figure 4 shows the half amplitudes of the first and second harmonics, which harmonics proved to be the only ones of any importance in the bending motion, plotted against tip-speed ratio, together with values from the PCA-2 autogiro for comparison. (See reference 1.) Figure 5 shows the phase angles for the XOZ-1.

Bending in the plane of rotation was not analyzed for the 1940 tests, because it was felt that a sufficient index of this item had been obtained from the 1939 data. Figure 6 shows the displacement of the tip in the plane of rotation plotted against azimuth for the best steady-flight run obtained in the 1939 tests. Corrections were made for the effect of feathering, using the feathering angle from the control-position indications, together with the position of the tip as obtained from the axial deflection and the built-in sweepback. The mean forward displacement of the tip is traceable to the eccentric tension loading which the centrifugal force exerts as a result of the plan form of the spar. It is evident that the blade covering may be stressed and distorted in a chordwise direction to an appreciable extent. It is also evident that the horizontal deflection does not add materially to the total stress in the blade spar.

Figure 7 summarizes the results of the feathering measurements after the use of harmonic analysis on the curves for the various runs. The equation on which the analysis was based is

$$\theta = A_o + A_1 \cos \psi + B_1 \sin \psi + A_2 \cos 2\psi$$
$$+ B_2 \sin 2\psi + \ldots$$

where θ, A_o, and the various coefficients have meanings corresponding to β, a_o, and the various coefficients in the flapping equation, but represent degrees pitch angle at the three-quarter radius instead of inches deflection at the tip. Harmonics other than the first were found to be small in comparison with the first; the second harmonic reached values of the order of 0.1°, but only at the higher tip-speed ratios, and the third, fourth, and fifth harmonics were still smaller. It will be noted that the mean value, A_o, of the feathering angle is, within the accuracy of the measurements, equal to the static pitch setting, or about 0.8°. It appears that a slight decrease in A_o occurs with increasing tip-speed ratio, but the amount is so small that the mean twist may be considered essentially zero at all speeds.

The difference between the amplitude of feathering as measured and the amplitude as calculated from the control-position record may be ascribed chiefly to blade twist. The difference indicates the approximate magnitude of this twist since, as is indicated in figure 8, the feathering applied by the controls and the actual or observed feathering are very nearly in phase. In this connection, the term twist includes not only torsional deflection in the blade spar, but also the effect of any deflection in the control linkages and bearing supports, since the control-position recorder is attached near the stick. In calculating the

increment of blade-root bending stress chargeable to use of the feathering control for trimming or maneuvering the machine, the increase in actual blade angle over that calculated from control deflection, that is, the twist as shown by the curves of figure 7, should be taken into account. On the other hand, the increment of stress so chargeable is dependent, not on the actual feathering, but only on the difference between the actual feathering and that which would produce zero pitching and rolling moments.

The data obtained from the instruments are summarized in figure 9. The stick force appears constant enough over the full range of tip-speed ratios covered to suggest that it could be made essentially zero by the use of a bungee. The near approach of the aileron deflection to zero at the higher speeds shows that the design precautions taken to achieve lateral balance, that is, (1) offset of lateral stick position for neutral feathering, (2) offset of rotor-control action in azimuth, and (3) twist used in the fixed wing, were successful. The elevator angle, however, bears out the pilot's contention that the ship was annoyingly tail-heavy, and shows that longitudinal balance was not properly taken care of at any forward speed in the range covered. A contributing factor in this improper balance is discussed later in this report.

The angle-of-attack curve cannot very well be used directly to determine the load distribution between the wing and the rotor, even if the scattered inclinometer data be discarded in favor of the horizon indications, because of the downwash or mutual interference between wing and rotor. The rotor rpm, however, together with the coning deflection of the blades as shown in figure 3, should give a fair indication which can then be checked by use of the angle of attack. Assuming that the lift of the rotor varies directly as its coning deflection for a given rpm, and as the square of its rpm for a given coning deflection, the load carried by the rotor at $\mu = 0.45$ is $(3.10/5.58)(164/210)^2$ or 0.34 as great as it is at $\mu = 0.175$. From this, it appears that the rotor is carrying rather less than one-third of the total load at $\mu = 0.45$, since it must have carried appreciably less than the full weight of the machine at $\mu = 0.175$. The order of magnitude of this value checks with the lift which may be calculated for the wing by using any reasonable downwash factor, together with the wing area, the dynamic pressure, and the angle of attack of the wing. In fact, by assuming a 2:1 ratio of lift between wing and rotor for the purpose of obtaining an equivalent aspect ratio, and using regular biplane theory, the fixed-wing load may be calculated as 1390 pounds, leaving 30 percent of the gross weight for the rotor, tail, thrust component, and other lift sources to carry, the rotor, of course, carrying the largest part.

Figure 10 shows the results of the tuft observations, with azimuth for stalling and unstalling plotted against μ. These data have been cross-plotted to give the outer boundaries of the stalled region for several tip-speed ratios in figure 11, and may be compared with figure 7 of reference 2. While the stalling on the gyroplane blades reaches somewhat larger radii than were found for the autogiro of reference 2, the areas are much narrower and the losses represented are probably smaller. It is not to be expected that the areas should be the same; the interference of the lower wing should change the shape of the gyroplane stalling boundary, and the lower pitch should reduce its size. The suppression of the coning angle should tend to narrow the region and to shift it somewhat. Further, the blade sections were different, and some change had been made in the technique of observation. Comparison of the gyroplane boundaries with others which have been more thoroughly analyzed leads to the conclusion that the stalled region on this rotor is not a factor of any real importance in the drag of the machine at any speed up to its top speed in level flight at least.

ACCURACY

Probable errors in the faired results are thought to be about as follows:

Airspeed, miles per hour	±1
Rotor speed, rpm	±2
Attitude angle, degree	±0.5

Elevator angle, degree	± 1
Aileron angle, degree	± 1
Control force, pound	± 1
Feathering coefficients, degree	± 0.1
Blade deflection in bending, inch	± 0.1
Phase angles, degrees	± 3
Stalled-area boundaries, degrees in azimuth	± 10

These values include errors in zero readings; the slopes of the curves should be more reliable. They do not include inconsistencies in the actual performance of the gyroplane caused by a change in air density or from any other source, but only errors in instrument calibration and response and in the working up of the data. It will be noticed that flight 3 does not duplicate flight 2, although the results are parallel. A partial explanation for this is that the rotor blades were cleaned off between the two flights.

DISCUSSION

The bending data obtained provide an interesting conclusion concerning the tail heaviness of the ship when consideration is given to the meaning of the existence of the first and second harmonic, respectively. First harmonic bending necessarily results in pitching or rolling moments, or both. Its existence in steady flight means that a rotor moment is present which affects the balance of the ship. If the ship were completely balanced by other means,

both fore and aft and laterally, the feathering, which is first harmonic, could be adjusted to entirely remove the first harmonic bending at any given condition of flight. Examination of figure 4 shows that the first harmonic bending would then be small over the entire range of flight speeds. The second harmonic bending cannot be affected by changing the feathering, unless second harmonic feathering is resorted to, neither does it affect the control moments at all. Its existence may be considered as caused by variations in downwash encountered by the blade during a revolution.

Examination of figures 4 and 5 will show that the first harmonic bending is such as to produce a positive pitching moment, that is, a moment tending to make the ship tail-heavy, over the entire range of speeds covered, with no indication of its disappearance should this range be exceeded in either direction, unless, perhaps, if vertical descent should be approached. Calculations show that the magnitude of this moment is such that it is a major factor in the balance of the ship. For example, at $\mu = 0.35$, the half amplitude is 1.9 inches at the tip, and the phase is essentially fore and aft. One inch change in tip deflection corresponds to some 330 foot-pounds change in moment at the roots of the blades under these conditions, hence the pitching moment of the four blade rotor is

$$(0.636)(1.9)(4)(330) = 1600 \text{ foot-pounds}$$

This is equivalent to moving the center of gravity of the ship 10 inches rearward, and must therefore represent a sufficient source for the annoying tail-heavy condition of the machine. Calculations, necessarily crude, of the negative pitching moment contributed by the horizontal tail surfaces gave an answer of the same order of magnitude as the positive pitching moment calculated for the rotor, although somewhat larger. It appears, therefore, that the ship would trim with elevators close to neutral if the feathering of the blades were adjusted to remove the rotor pitching moment. Some improvement in performance and general handling characteristics would also result, since in the present arrangement the tail and the rotor are working against each other in achieving balance. Maximum blade stress would be reduced, both during steady flight and during maneuvers.

The sources of the fore-and-aft bending include (1) difference in the downwash angle of the air met by the blade when ahead and when behind, and (2) lag in the bending deflection of the blade after the forces causing it, which means that the effect of any excess of lift on the advancing side over that on the retreating side, although taken care of by blade inertia at the point where it occurs, will be felt as a control moment at a later phase angle, when the deflection has had time to build up. Judging from the control advance found necessary, this rotor has a lag of some 30° between applied

force and resulting deflection. It is hardly conceivable that item (1) could ever disappear completely. Item (2) approaches zero as the blades approach infinite rigidity, since both the phase lag and the bending motion approach zero. Since there are advantages in having some flexibility, this factor is not likely completely to disappear either. It may be concluded, therefore, that the tendency toward fore-and-aft unbalance should be given consideration almost on a par with the tendency toward lateral unbalance when deciding on the initial feathering or feathering with controls neutral to be used in any machine with a nonarticulated rotor.

While the second harmonic does not affect balance and control, it is a source of blade-bending stress, and its rapid rate of rise at the upper end of the speed range (see fig. 4), together with the fact that it has reached a value larger than the first harmonic, suggests that large blade stresses might be encountered before the rotor could be completely unloaded. It is curious that the second harmonic should be just as large as that for the hinged rotor of the PCA-2 (see fig. 4), while the first harmonic is greatly subdued, and it was thought that the natural frequency of the gyroplane blades might be amplifying the second harmonic but not the first. While this factor may have contributed, it appears not to be the major item, because (1) no abrupt phase shift occurs, unless perhaps at the lowest tip-speed ratios (fig. 5), and (2) when the values are plotted against

rpm (see fig. 12), flights 2 and 3 separate distinctly, whereas they blend together when plotted against tip-speed ratio (see fig. 4), showing that rpm is not the controlling factor which it would be if natural frequency were responsible for the phenomenon in question. One reason for the relative size of the first and second harmonics of bending is, of course, the reduction of the first harmonic by feathering.

The bending data taken at the various radii can be cross-plotted to give the blade-bending curve for a given azimuth at a given tip-speed ratio. Figures 13 and 14 illustrate the nature of the curves so obtained. While the accuracy is insufficient to warrant detailed calculation of blade stress and loading distribution, it is clearly evident that the outer 40 percent of the blade is very nearly a straight line; apparently, the centrifugal loads and the air loads are almost balanced on this portion of the blade. The straightness of the outer portion also means that if the root stress should be calculated from tip deflection on the assumption of a parabolic curve in the blade spar, the calculated stress would be less than the actual.

CONCLUSIONS

1. A rotor of the nonarticulated type, if used in translation, should be given an initial feathering, not only for lateral balance, but also for longitudinal balance.

2. The annoying tail heaviness of the XOZ-1 resulted in large measure from the rotor pitching moment and could have been prevented by using an additional initial feathering similar to that successfully used to achieve lateral balance but applied 90° later in azimuth.

3. Control forces and stick vibration in the XOZ-1 gyroplane are reasonable in magnitude.

4. Blade-tip deflection of the XOZ-1 rotor reaches a maximum value of the order of $7\frac{1}{2}$ inches in steady flight over the range of speeds covered, namely from 39 to 79 miles per hour.

5. Second harmonic forces exist in the XOZ-1 gyroplane rotor which are rapidly becoming important relative to blade stress as the highest speeds are reached.

6. Observed blade feathering in the XOZ-1 gyroplane rotor reaches a half amplitude of 2.6° at $\mu = 0.45$.

7. Periodic twist accounts for 0.5° of this 2.6° feathering; mean twist is essentially zero.

8. Observed blade feathering in the XOZ-1 gyroplane rotor is almost entirely first harmonic.

9. Rotor blade-section stalling is not an important factor in the drag of the XOZ-1 gyroplane up to its top speed in level flight.

10. The rotor of this gyroplane was successfully unloaded in these tests to the extent of carrying one-third or less of the weight of the machine.

Langley Memorial Aeronautical Laboratory,
National Advisory Committee for Aeronautics,
Langley Field, Va., September 12, 1941.

Frederic B. Gustafson
Frederic B. Gustafson,
Assistant Aeronautical Engineer.

EWM 9/19

Approved:
Elton W. Miller,
Head Mechanical Engineer.

MHY

REFERENCES

1. Wheatley, John B.: An Aerodynamic Analysis of the Autogiro Rotor with a Comparison between Calculated and Experimental Results. Rep. No. 487, NACA, 1934.

2. Bailey, F. J. Jr., and Gustafson, F. B.: Observations in Flight of the Region of Stalled Flow over the Blades of an Autogiro Rotor. T. N. No. 741, NACA, 1939.

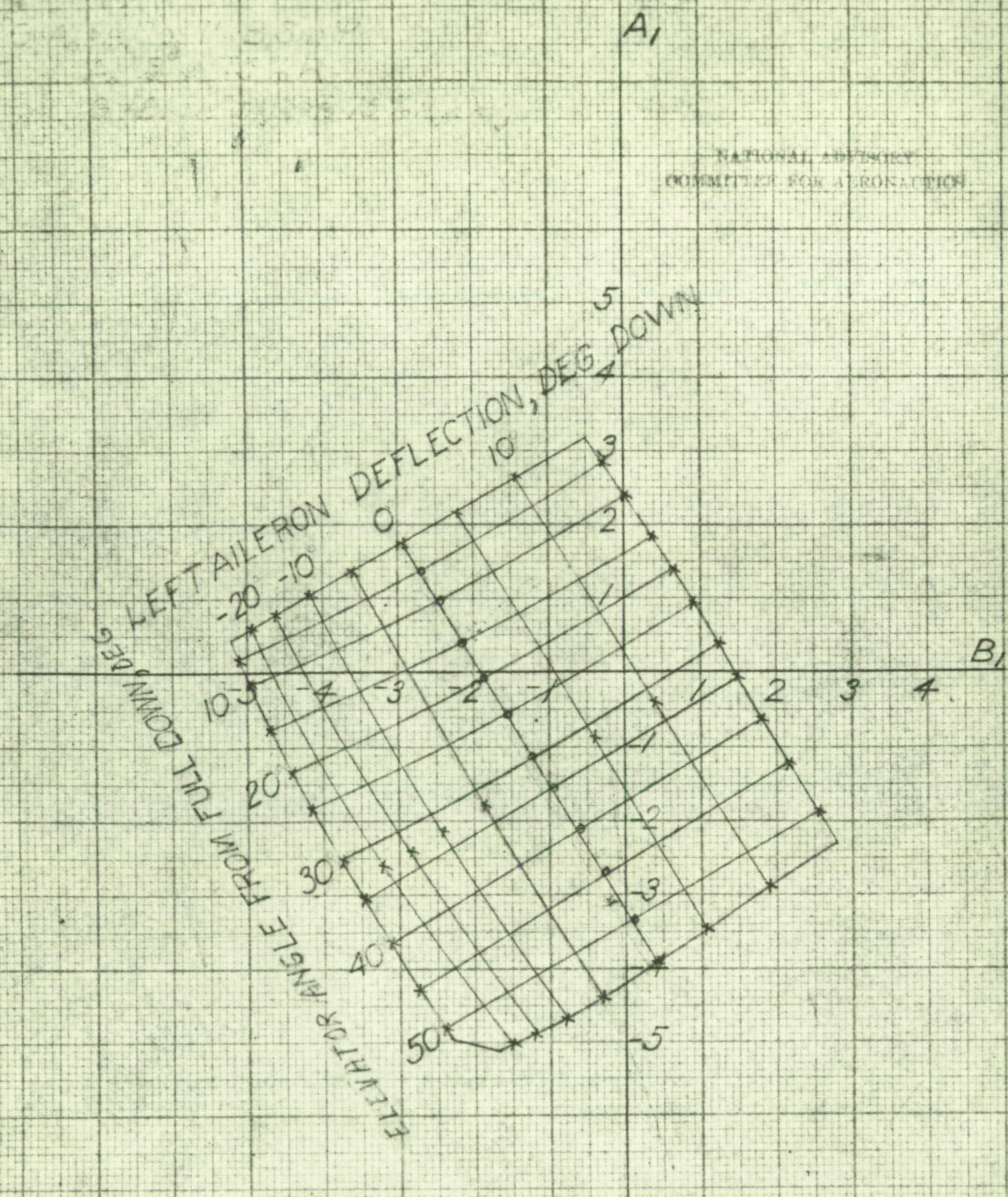

Figure 1. - Relation between elevator and aileron positions and blade feathering; XOZ-1 gyroplane rotor. θ, blade angle at 0.75R, degrees; $\theta = A_o + A_1 \cos \psi + B_1 \sin \psi$; $A_o = 0.8^\circ$ at 0.75R.

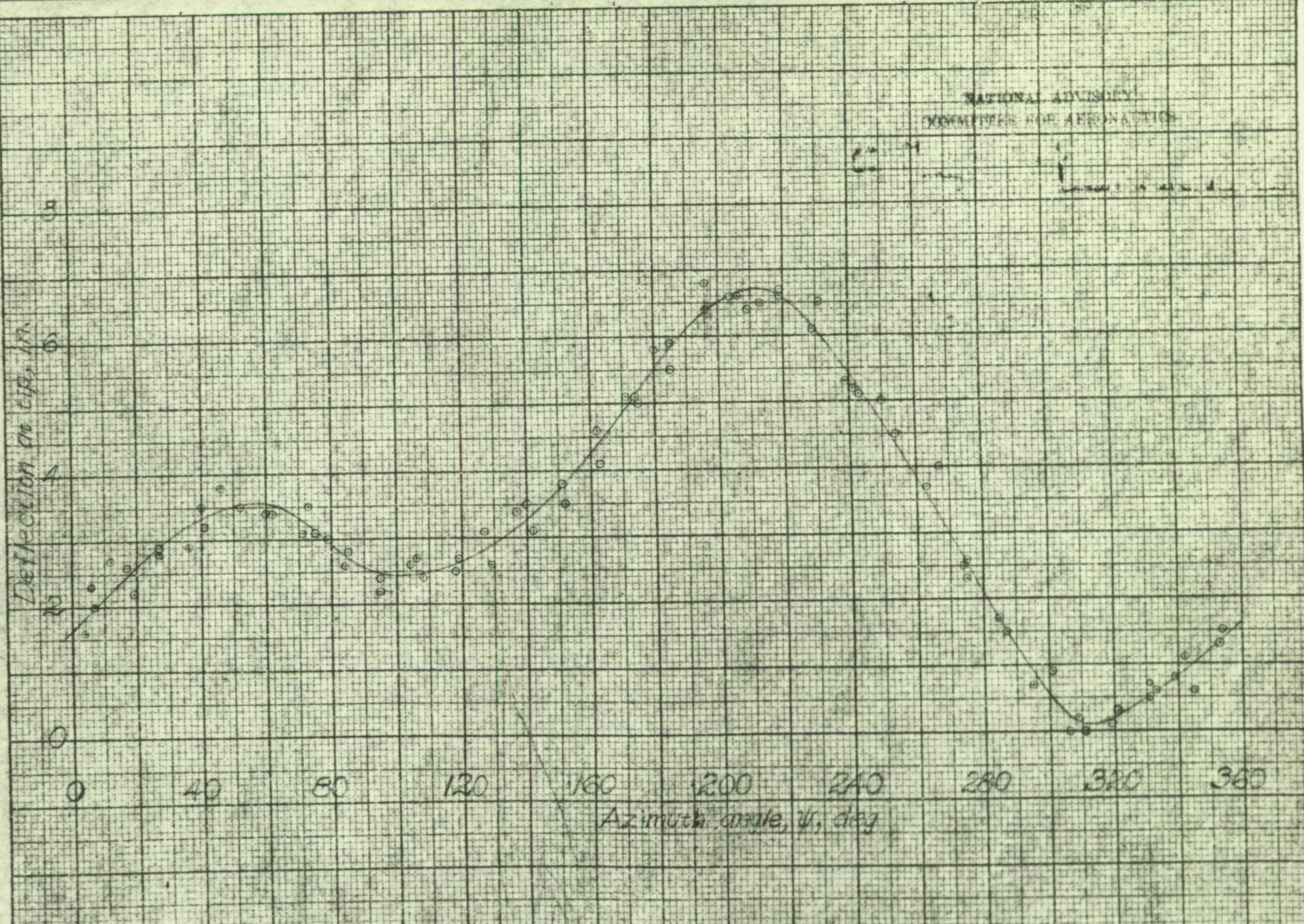

Figure 2. - Sample of plot of corrected blade bending-deflection data obtained from each run at each radius; XOZ-1 gyroplane rotor. $\mu = 0.39$.

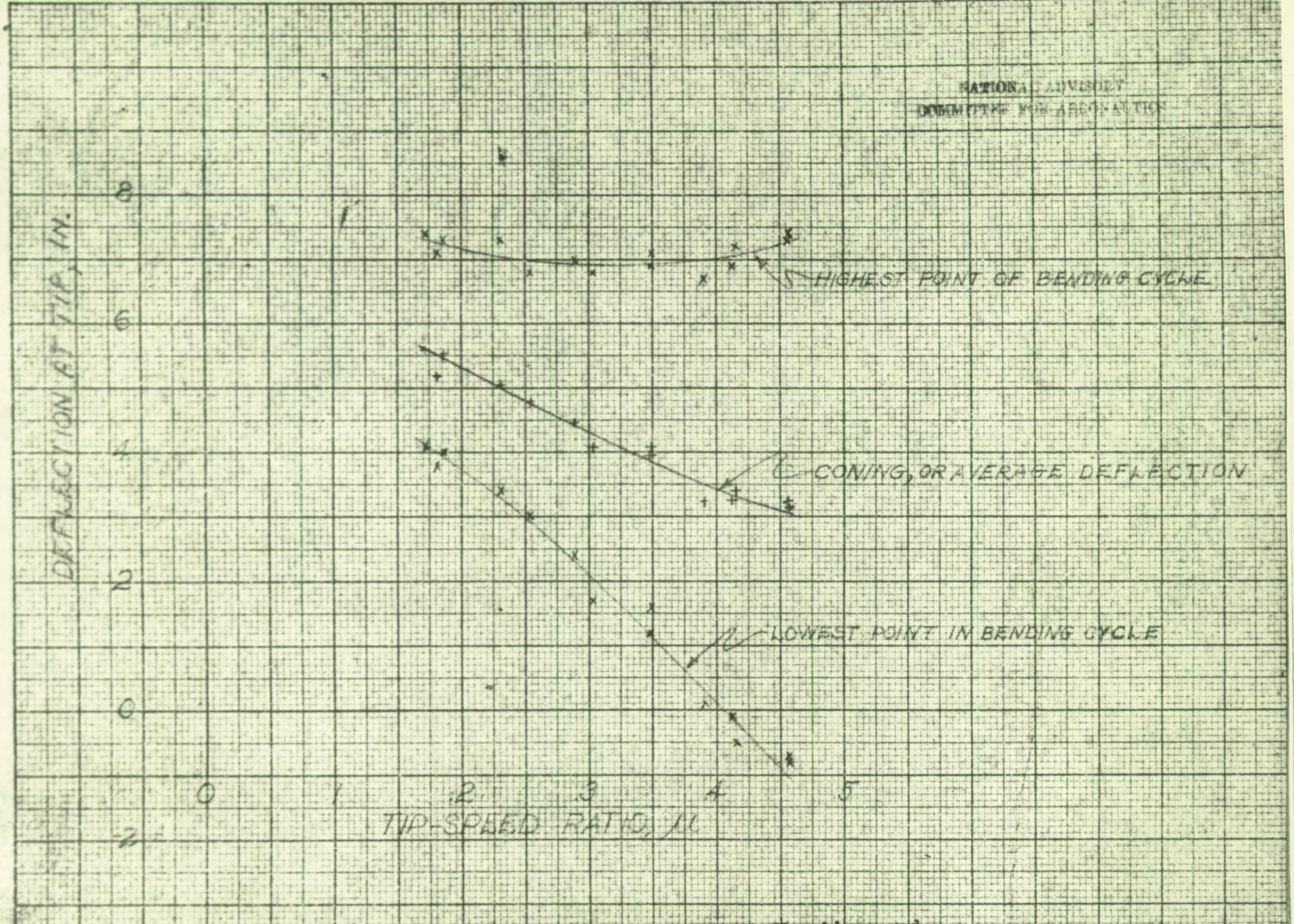

Figure 3. - Average blade-tip or coning deflection and high and low points of bending plotted against tip-speed ratio; XOZ-1 gyroplane rotor.

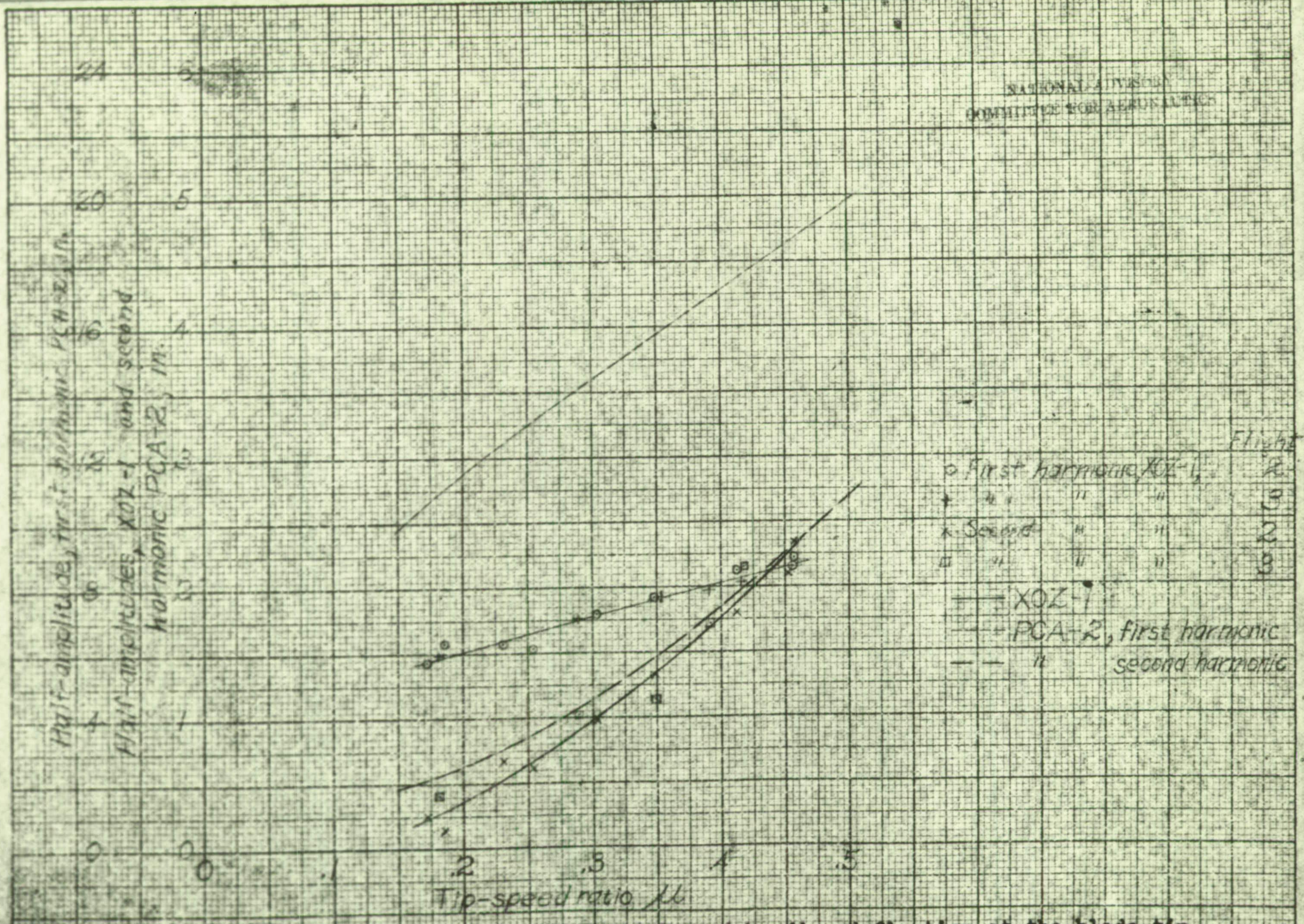

Figure 4. - First and second harmonics of bending deflection at the blade tip plotted against tip-speed ratio for the XOZ-1 gyroplane. Values for the PCA-2 autogiro rotor at 180 inches radius are included for comparison.

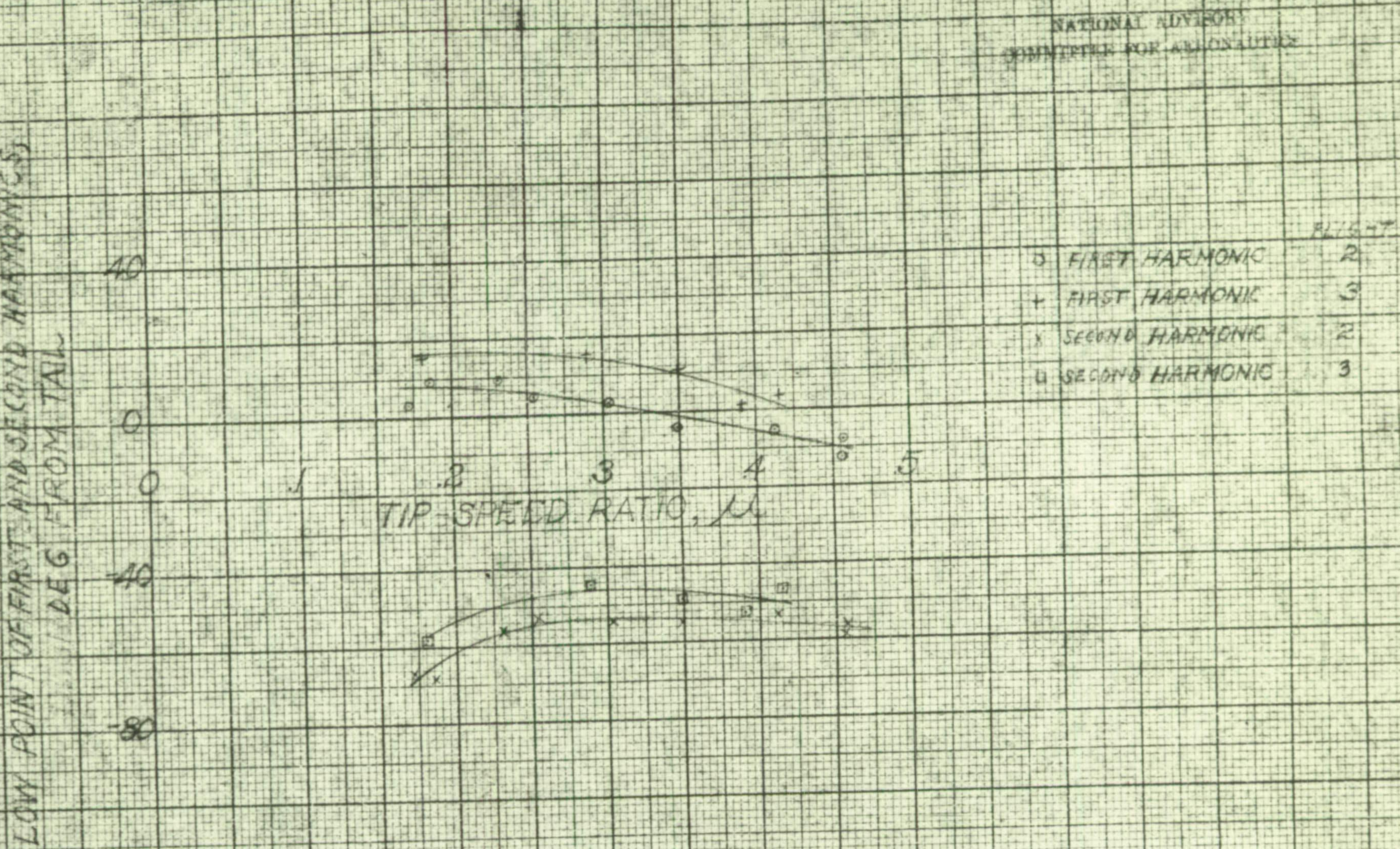

Figure 5. - Phase angles for low points of bending cycles plotted against tip-speed ratio; XOZ-1 gyroplane rotor.

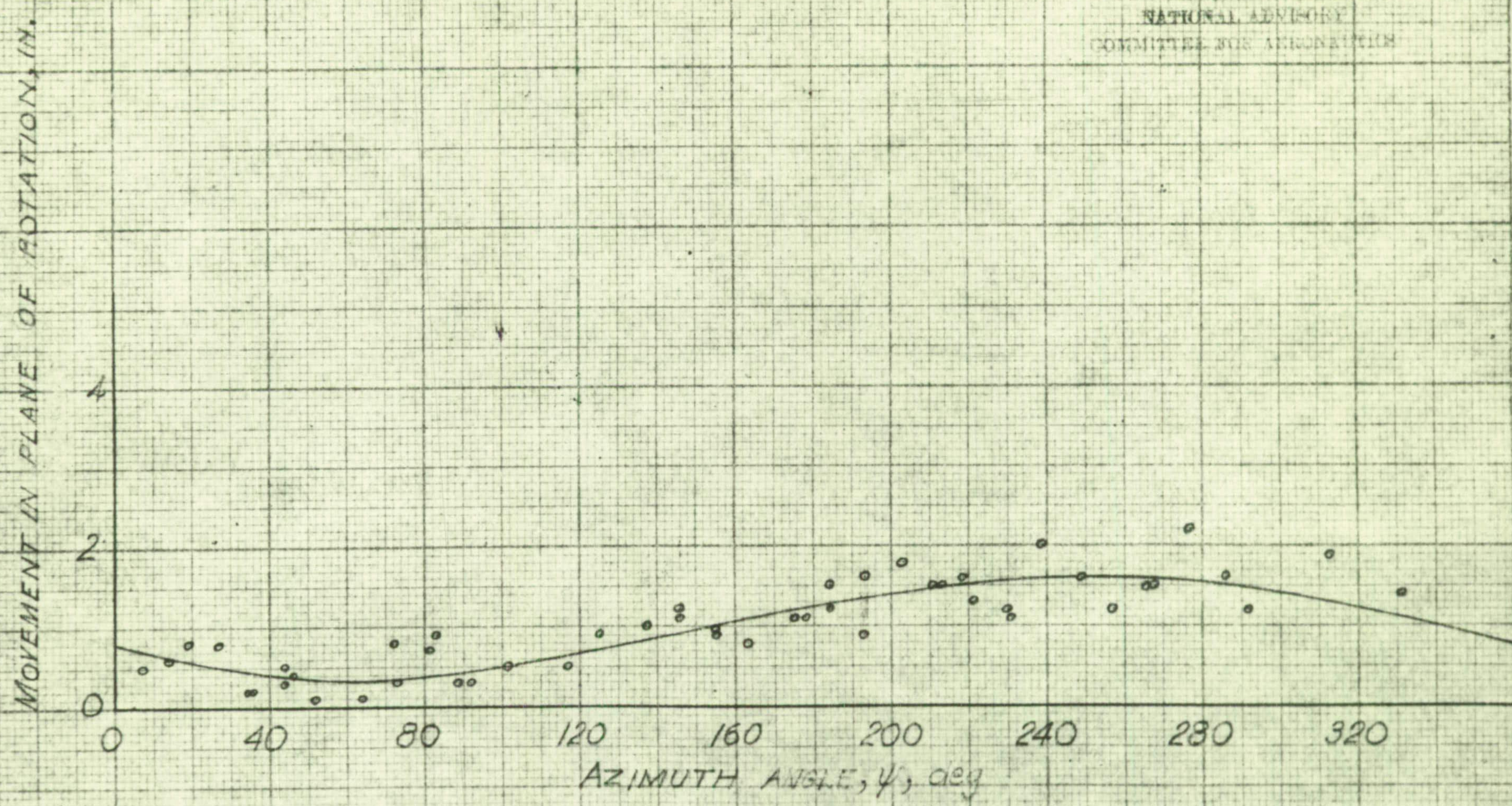

Figure 6. - Bending displacement of tip of blade in plane of rotation plotted against azimuth for $\mu = 0.30$; XOZ-1 gyroplane rotor.

6.

PRINTED IN U.S.A.

EUGENE DIETZGEN CO. NO. 346 B

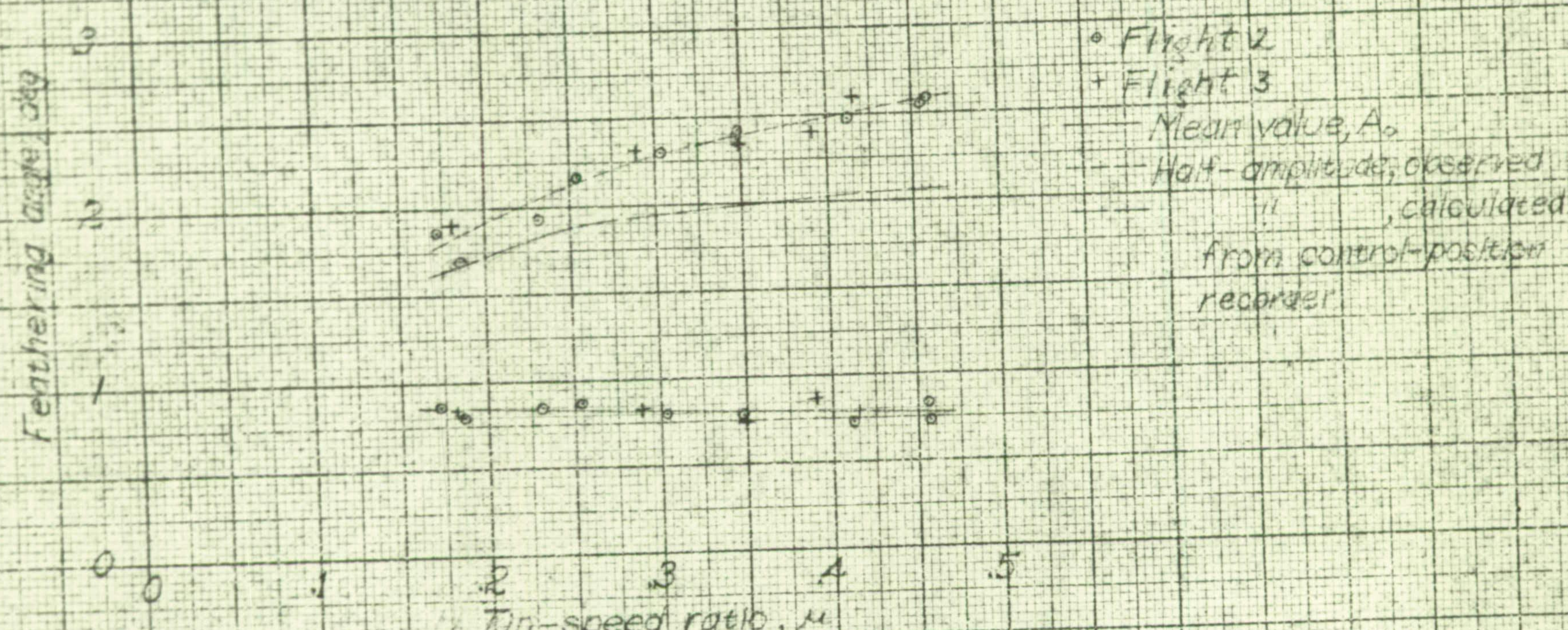

Figure 7. - Feathering values plotted against tip-speed ratio; XOZ-1 gyroplane rotor.

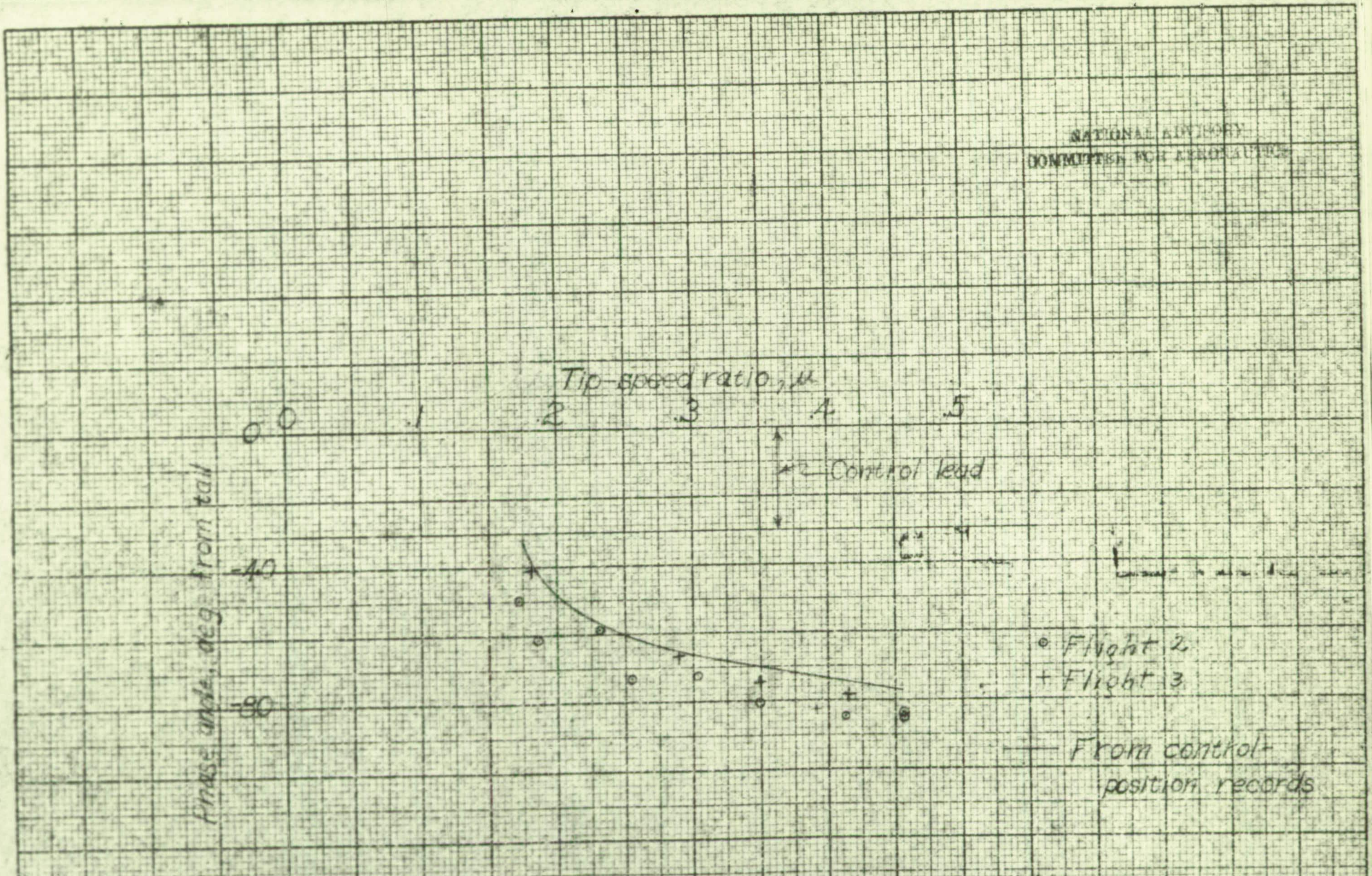

Figure 8. - Phase angles for high points of feathering cycles plotted against tip-speed ratio; XOZ-1 gyroplane rotor.

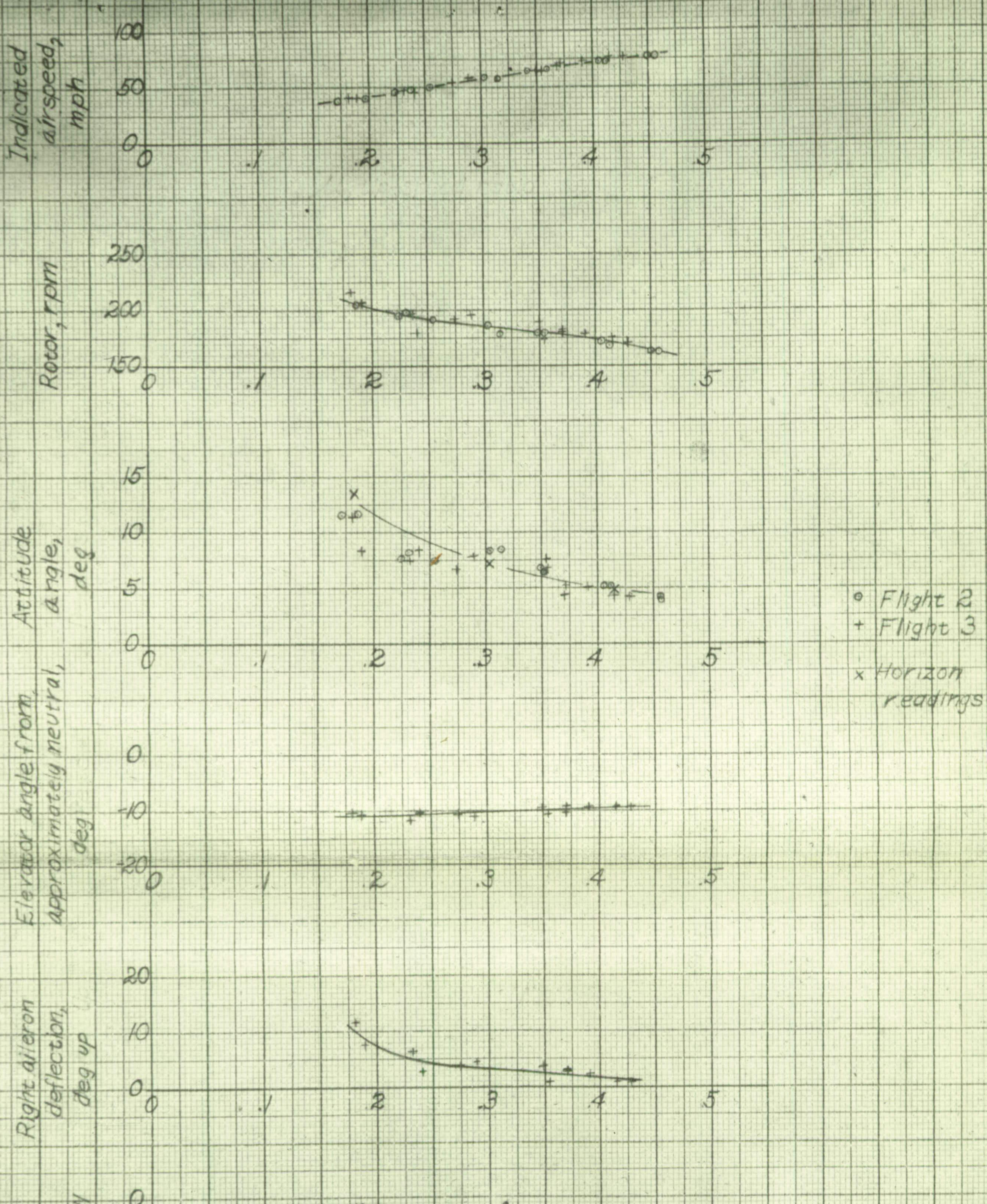

Figure 9. - Data obtained from instrument records plotted against tip-speed ratio; XOZ-1 gyroplane rotor.

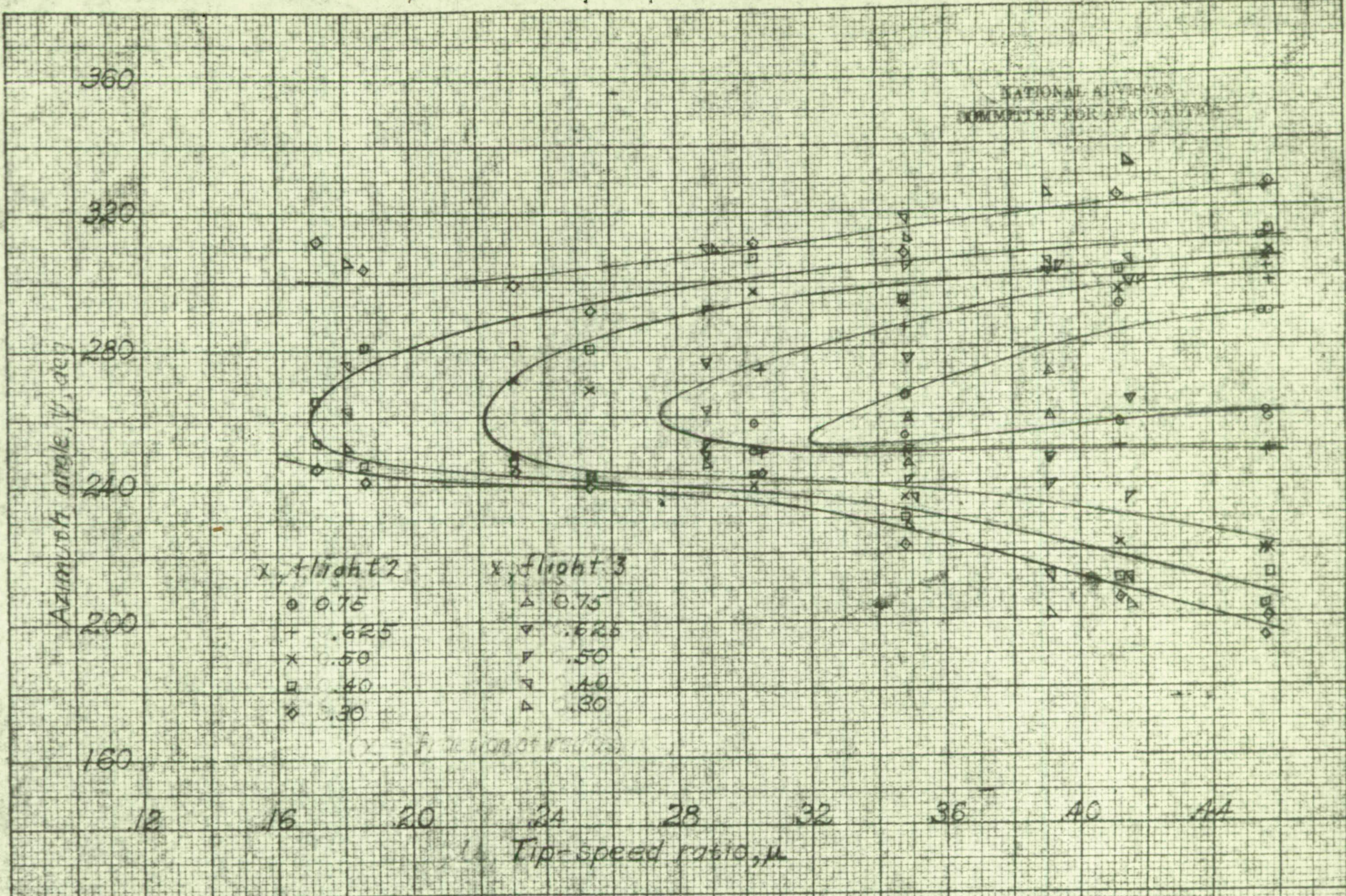

Figure 10. - Azimuth for stalling and unstalling of blade elements plotted against tip-speed ratio; XOZ-1 gyroplane rotor. X, fraction of radius.

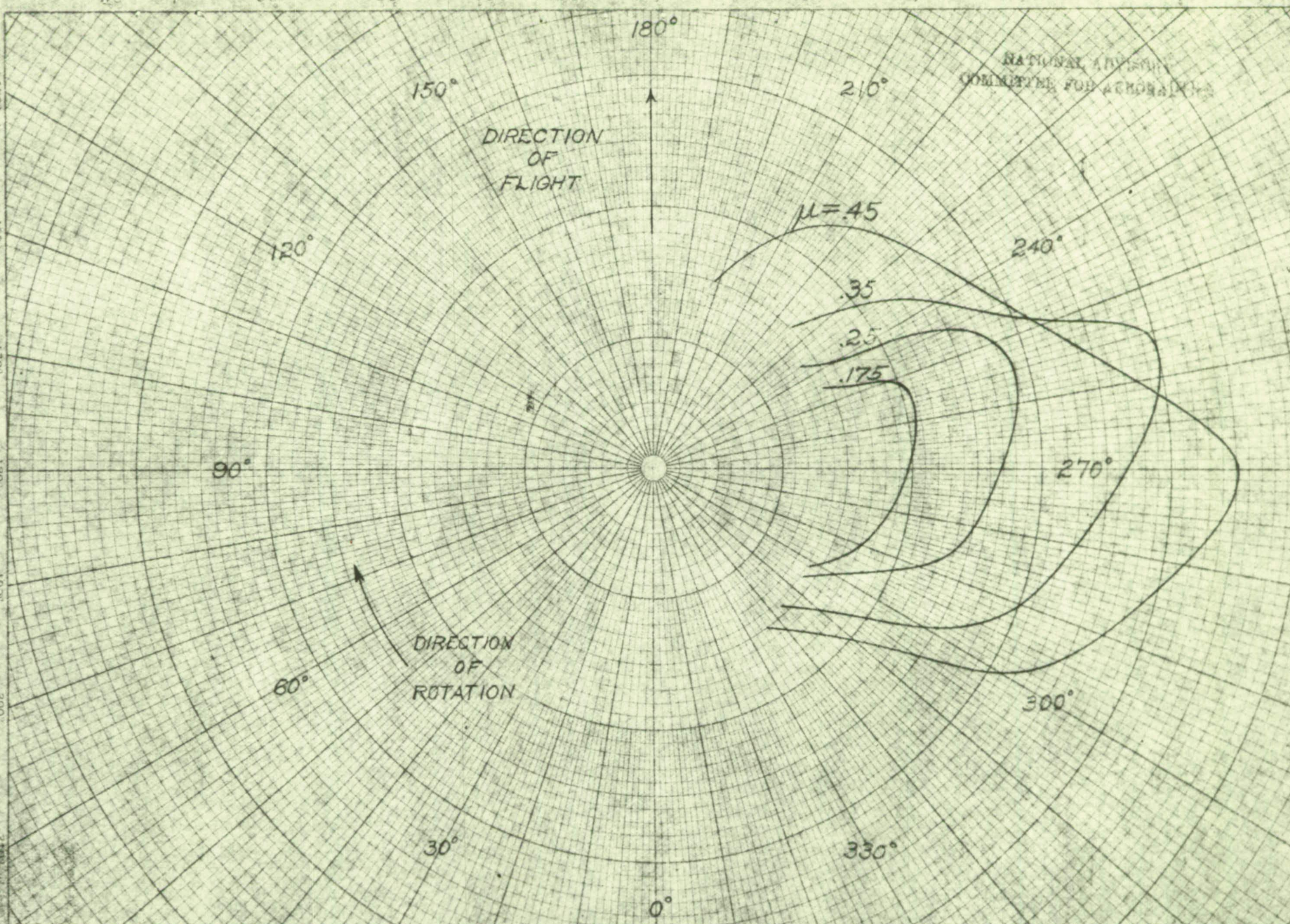

Figure 11. - Outer boundaries of stalled region for several tip-speed ratios; XOZ-1 gyroplane rotor.

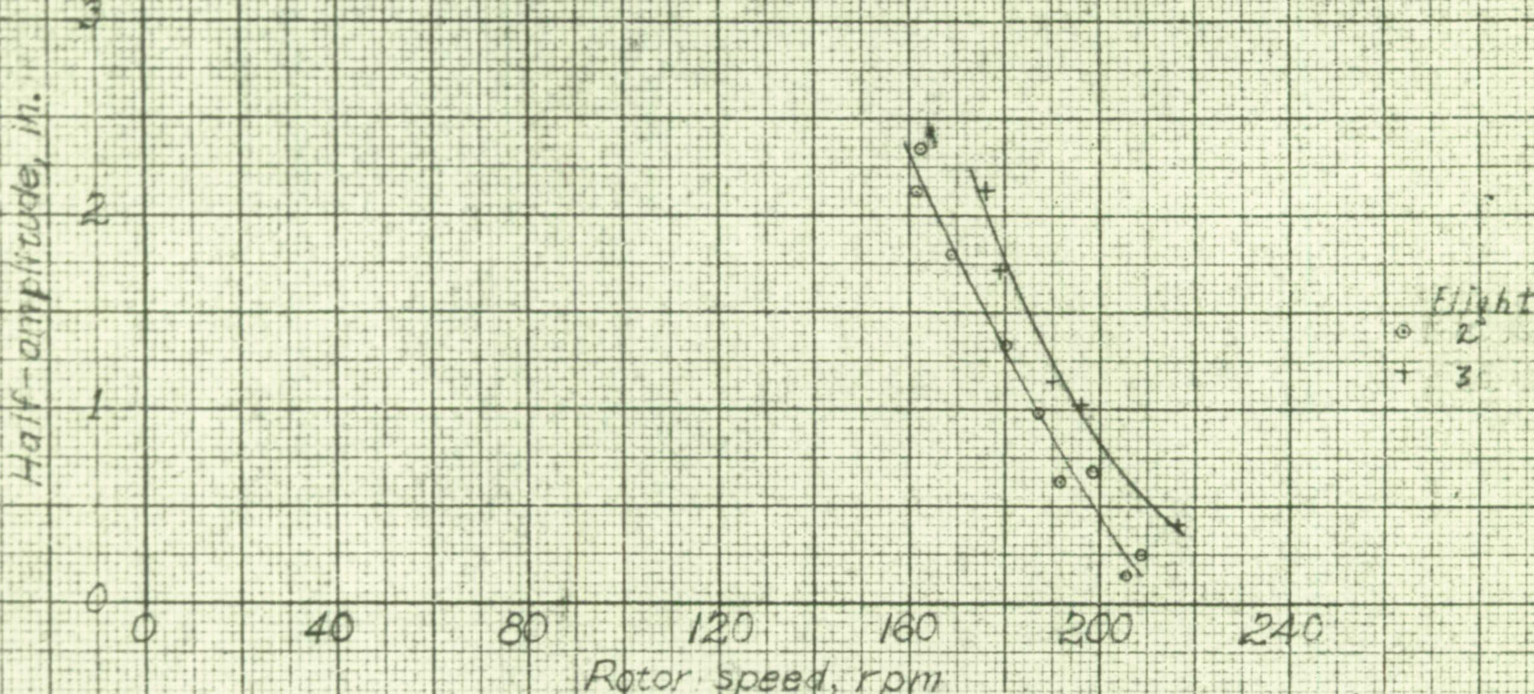

Figure 12. - Second harmonic blade-bending amplitude plotted against rotor spin; XOZ-1 gyroplane rotor.

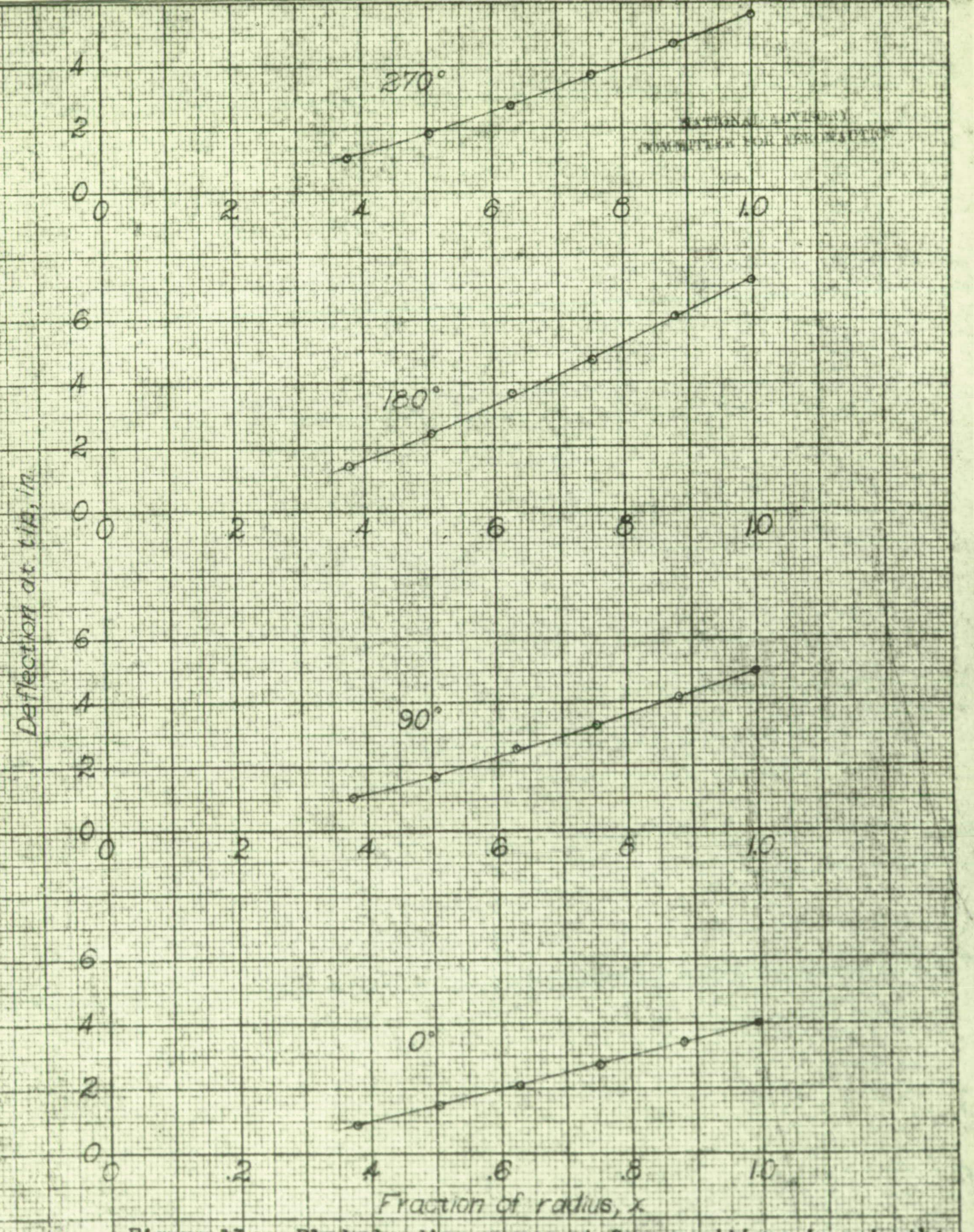

Figure 13. - Blade-bending curves at four positions in azimuth; XOZ-1 gyroplane rotor.
(a) μ, 0.18

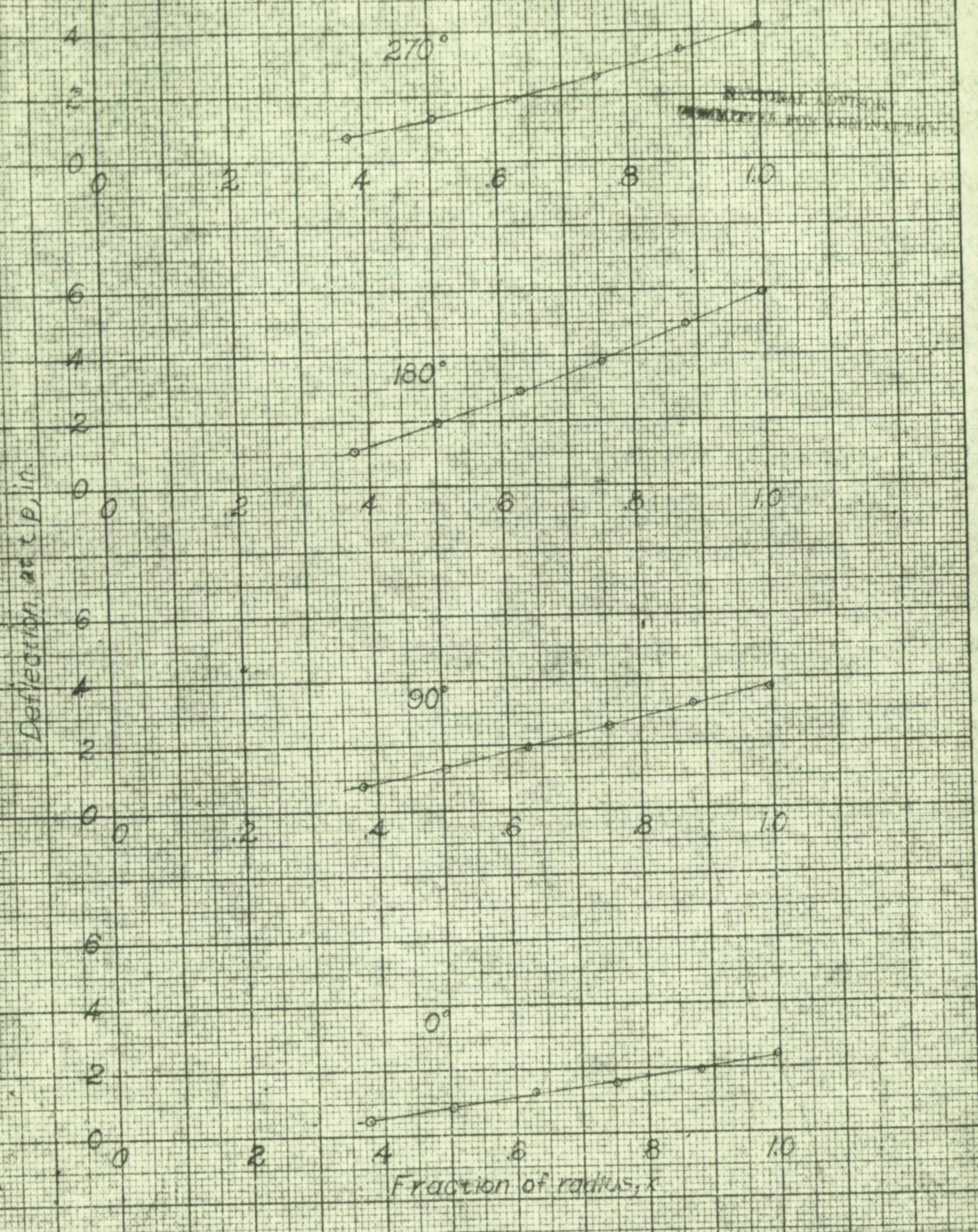

Figure 13(b)
μ, 0.30.

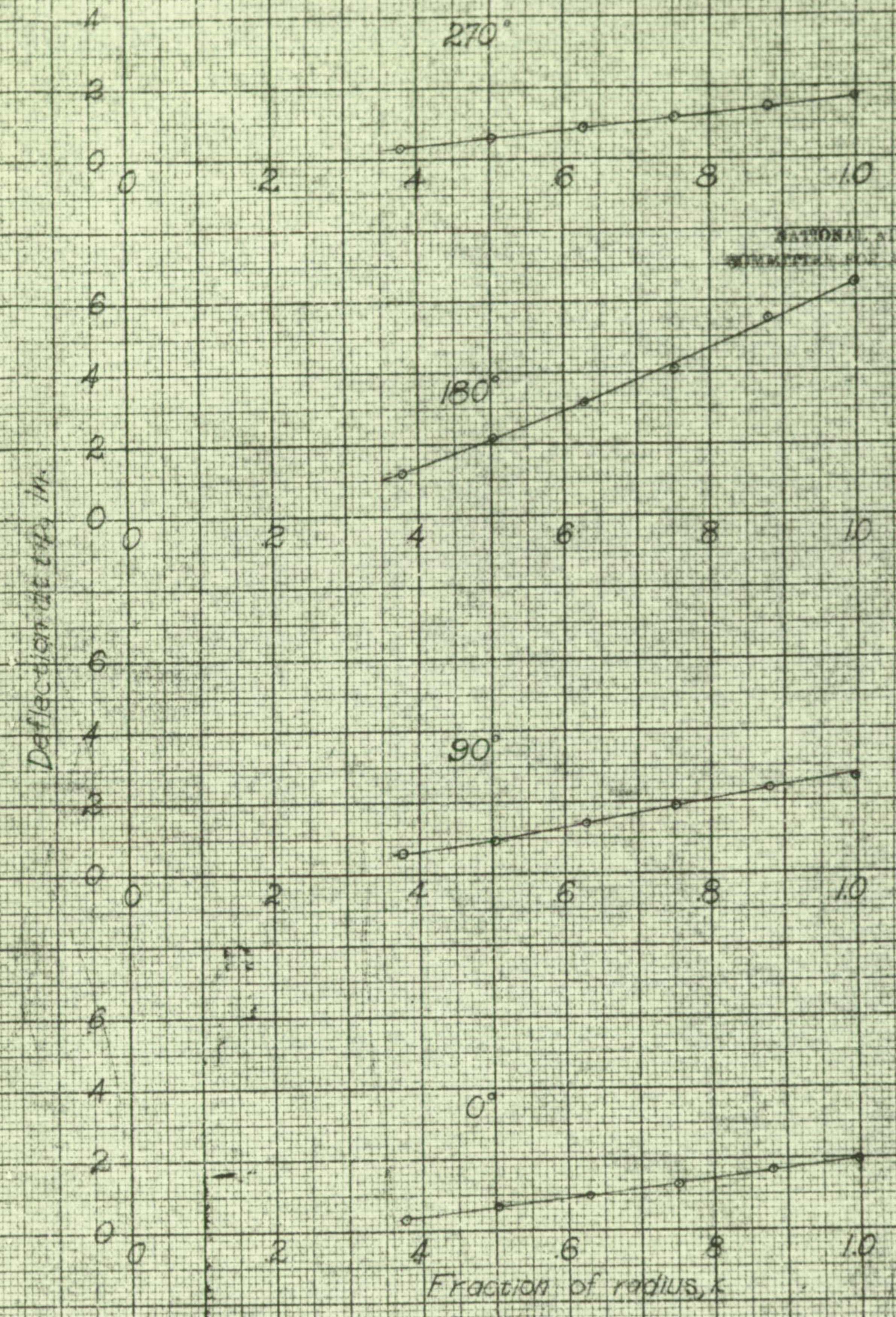

Figure 13(c)
μ, 0.46.

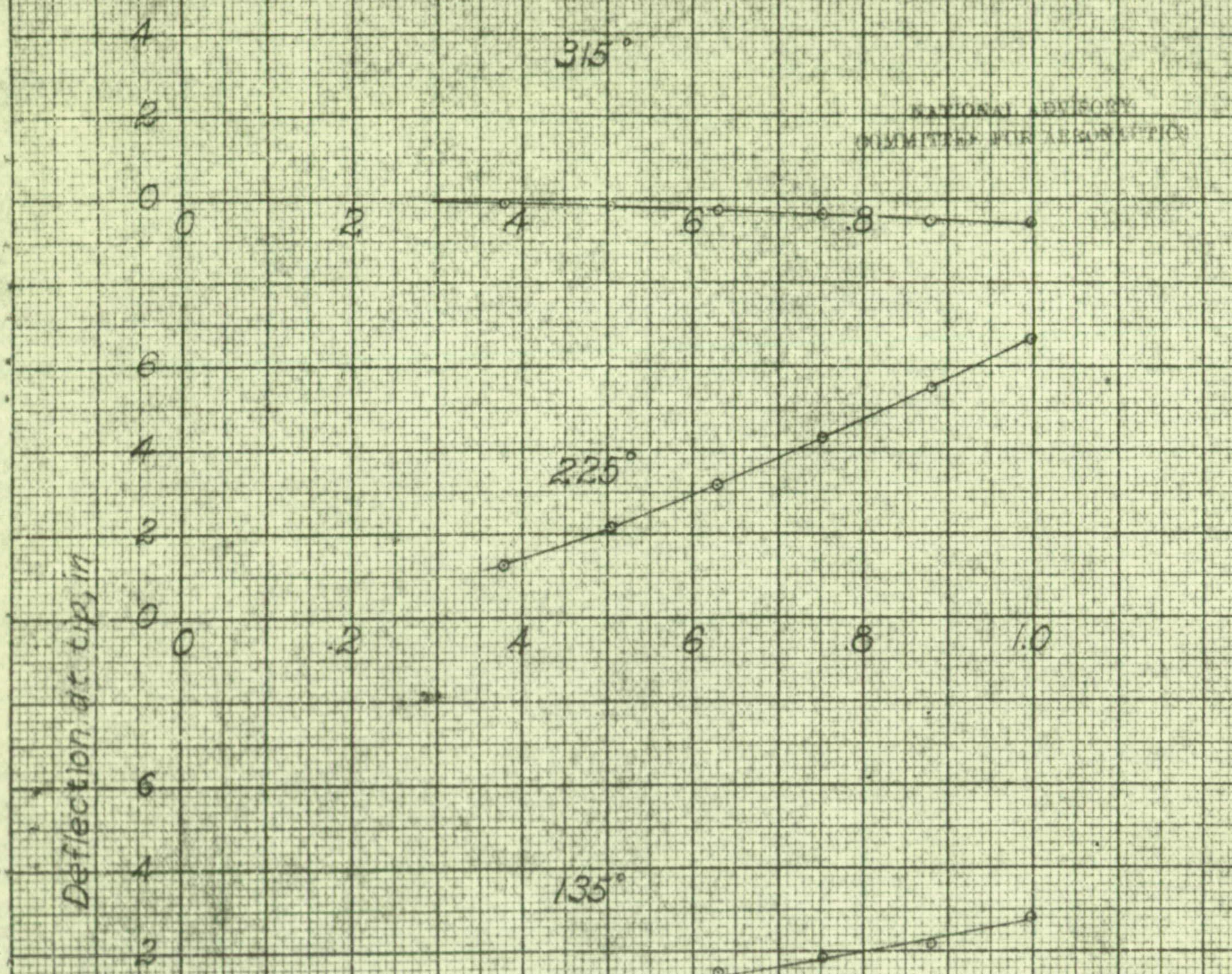

Figure 14. - Blade-bending curves for $\mu = 0.46$ at four positions intermediate to those of figure 13(c).